Received: 31 May 2020 | Revised: 14 July 2020 | Accepted: 24 July 2020
DOI: 10.1002/qua.26436

FULL PAPER

International Journal of QUANTUM CHEMISTRY WILEY

Density functional theoretical tailoring of electronic effect through various substituents on calix[4]arene-crown-6 for efficient Cs^+ ion encapsulation and extraction

Anil Boda | Sk. Musharaf Ali

Chemical Engineering Division, Chemical Engineering Group, Bhabha Atomic Research Centre, Mumbai, Maharashtra, India

Correspondence
Sk. Musharaf Ali, Chemical Engineering Division, Chemical Engineering Group, Homi Bhabha National Institute, Mumbai 400 085, Maharashtra, India.
Email: musharaf@barc.gov.in

Abstract

The structure, energetic, and quantum chemical descriptors of Cs^+ complexes of calix[4]arene-crown-6 (C4C6) and substituted C4C6, that is, 1,3 alternate-diethoxy C4C6, are reported here based on the analysis of results obtained using density functional theory (DFT). Substitution of benzo group in both C4C6 and 1,3 alternate-diethoxy C4C6 resulted in a reduction of binding energy (BE). Further substitution of the benzo group with methyl, methoxy, and amino groups leads to an increase in BE, and nitro substitution leads to decrease in BE for C4C6, whereas in the case of 1,3 alternate-diethoxy calix[4]arenebenzocrown-6, methoxy substitution leads to the highest BE compared to other complexes. The calculated Gibbs free energy, ΔG_{gas} also followed the same order as BE in the case of 1,3 alternate-diethoxy C4C6 and their substituted ligands. Furthermore, the ΔG of complexation was computed using a thermodynamic cycle with conductor-like screening model in different solvents: toluene, chloroform, octanol, and nitrobenzene. The values of ΔG_{ext} are found to be increased with an increase in the dielectric constant of the solvent and were found to be highest in the nitrobenzene. The atoms in molecule analysis reveals partial ionic character in the Cs—O bond. Among all the studied complexes, 1,3 alternate-diethoxy calix[4]arene 3′-methoxy benzo crown-6 displays highest ΔG_{ext} in nitrobenzene. The calculated value of $\Delta\Delta G_{ext}$ ($\Delta\Delta G = \Delta G_{Cs+} - \Delta G_{Na+}$) is found to be –41.82 kcal/mol with 1,3 alternate-diethoxy calix[4]arene 3′-methoxy benzocrown-6, which is higher than that obtained with calix [4] bis-crown-6 (−5.24 kcal/mol). The newly designed ligand might be suitable for the selective extraction of Cs^+ over Na^+ in the reprocessing of nuclear waste and thus invites experimentalists to test this DFT finding in the laboratory.

KEYWORDS
binding energy, calix[4]arene-crown-6, cesium, DFT, free energy

1 | INTRODUCTION

Calixarenes and the derivatives of calix[4]arene have drawn considerable interest because of their strong ability to bind Groups I and II metal cations selectively in comparison to crown ethers.[1–3] Reprocessing of used nuclear fuel results in the long-lived Cs-137 fission product, which needs to be selectively separated from waste solutions containing high sodium ions.[4,5] Still, efforts are underway worldwide to devise a

molecular system to extract the Cs^+ ion from spent nuclear waste.[1,6–10] Crown ethers[11] and calix[n]arenes[12] have shown considerable interest for the selective extraction of Cs ion from spent nuclear waste. Furthermore, calixarene derivatives are also used in the cesium ion-selective electrodes.[13] The calix moiety alone has very weak attraction for cation (dipole-ion interaction); however, it can be electronically tailored by suitably functionalization.[14] Previous studies have shown that, for the selective extraction of Cs^+ extraction, crown ether attached to the 1,3-alternate conformation of calix[4]arene is the most favorable.[15,16] Several modifications to this calix[4]arene were reported, which includes calix[4]arene-bis-crown ethers,[7] dialkoxy calix[4]arene-mono-crown ethers,[15,16] and benzo and naphtho substituents on the crown ether of calix[4]arene[7,17,18] and n-octyloxy/n-propyloxy/iso-propyloxy- calix[4]arene monocrown ethers.[15,16] In order to have a better understanding of the electronic effect of substituents for the selective extraction, Sachleban et al. reported the Cs ion extraction with 12 different 1,3-alt calix[4]arene crown ethers in 1,2-dichloroethane diluent.[19] They noticed a remarkable increase in selectivity when a hybrid calix[4]arene biscrown ether molecule was used,[19] thus encouraging further exploration of new ligands. From the available solvent extraction experimental results,[20] the cation-ligand complexation reaction was established to be 1:1 as follows:

$$M^+_{(aq)} + L_{(org)} \xrightarrow{\Delta G_{ext}} M^+ - L_{(org)} \quad (1)$$

The Gibbs free energy of extraction, ΔG_{ext}, can be estimated for the above complexation reaction using a standard thermodynamic approach. The six ethereal O atoms and benzene rings of the calix structure are responsible for the increase in selectivity of Cs^+ ion.[16,21] Earlier, several density functional theory (DFT),[22–32] resolution of identity-Moller-Plesset (RI-MP2),[33] and molecular dynamics (MD)[34–36] studies were conducted to understand the Cs^+ ion complex with calix-crown systems. We have also previously studied the high selectivity of Cs^+ ion over Na^+ with calix[4]arene-biscrown-6[28] using DFT. In the present report, we extend our earlier study to investigate the electronic effect of different substituents on the calix[4]arene-crown for its complexation ability toward Cs^+ ion.

In this article, we report the structure and complexation of Cs^+ with calix[4]arene crown-6 and 1,3-diethoxy calix[4]arene crown-6 and their substituents, namely, benzo, methylbenzo, methoxybenzo, aminobenzo, and nitrobenzo, using DFT. The conductor-like screening model (COSMO) solvation approach was used to account for the solvent effect of water and organic solvent. Details of the computational methodology and results are described in the following sections.

2 | COMPUTATIONAL METHODOLOGY

The geometries of different chemical species were optimized, and total energies were calculated with the B3LYP functional[37,38] using a triple zeta valence plus polarization (TZVP) basis set, that is, C (11s6p1d)/[5s3p1d], O (11s6p1d)/[5s3p1d], H (5s1p)/[3s1p], and Cs (7s6p)/[5s3p]. Effective core potential was used for Cs with 46 core electrons. The hybrid B3LYP functional was better in predicting the energetics of several systems.[39] All the calculations were performed using the Turbomole suite of programs.[40] The aqueous and organic solvent effects in the energetics were included using the COSMO[41,42] model, which was found to be successful in predicting accurate solvation-free energy of the metal ions.[43] The dielectric constant, ε, of water and organic solvents, namely, toluene, chloroform, octanol, and nitrobenzene, were taken as 80, 2.38, 4.80, 10.38, and 34.82, respectively. It has been observed that the optimized geometries in the solvent phase have little effect on the solvation energy compared to single-point solvation energy using gas phase geometry.[28,44–50] Therefore, for the single-point energy calculation in COSMO phase, the geometries obtained from the gaseous phase were used. The computation of metal ion solvation energy is described elsewhere.[28] Furthermore, single-point energy calculations were performed using the optimized structures of B3LYP/TZVP with M06 functional,[51] using the TZ2P basis set for complimentary validation of methodology using the amsterdam density functional (ADF) package.[42,52]

3 | RESULTS AND DISCUSSION

3.1 | Structure of C4C6 and substituted C4C6 and their Cs^+ ion complexes

The optimized structures of C4C6 and substituted C4C6 are displayed in Figure 1, and the structural parameters are given in Table 1. The ligands of interest are calix[4]arene-crown-6 ($C_{38}H_{42}O_8$), hereafter called **I**; calix[4]arenebenzocrown-6 ($C_{42}H_{42}O_8$), **II**; calix[4]arene-3′methylbenzocrown-6 ($C_{43}H_{44}O_8$), **III**; calix[4]arene-3′methoxybenzocrown-6 ($C_{43}H_{44}O_9$), **IV**; calix[4]arene-3′aminobenzocrown-6 ($C_{42}H_{43}NO_8$), **V**; and calix[4]arene-3′nitrobenzocrown-6 ($C_{42}H_{41}NO_{10}$), **VI**, and the corresponding complexes with Cs^+ metal ion are **Ia**, **IIa**, **IIIa**, **IVa**, **Va**, and **Via**, respectively.

In the case of **I**, the C_{sp}^2 and O bond distances are 1.366 Å and 1.388 Å, whereas C_{sp}^3 and O bond distances are in the range of 1.414 to 1.431 Å. The diagonal O—O bond distances are also given in Table 1. In the complex, **Ia**, the C_{sp}^2 and O bond distances are increased to 1.382 Å

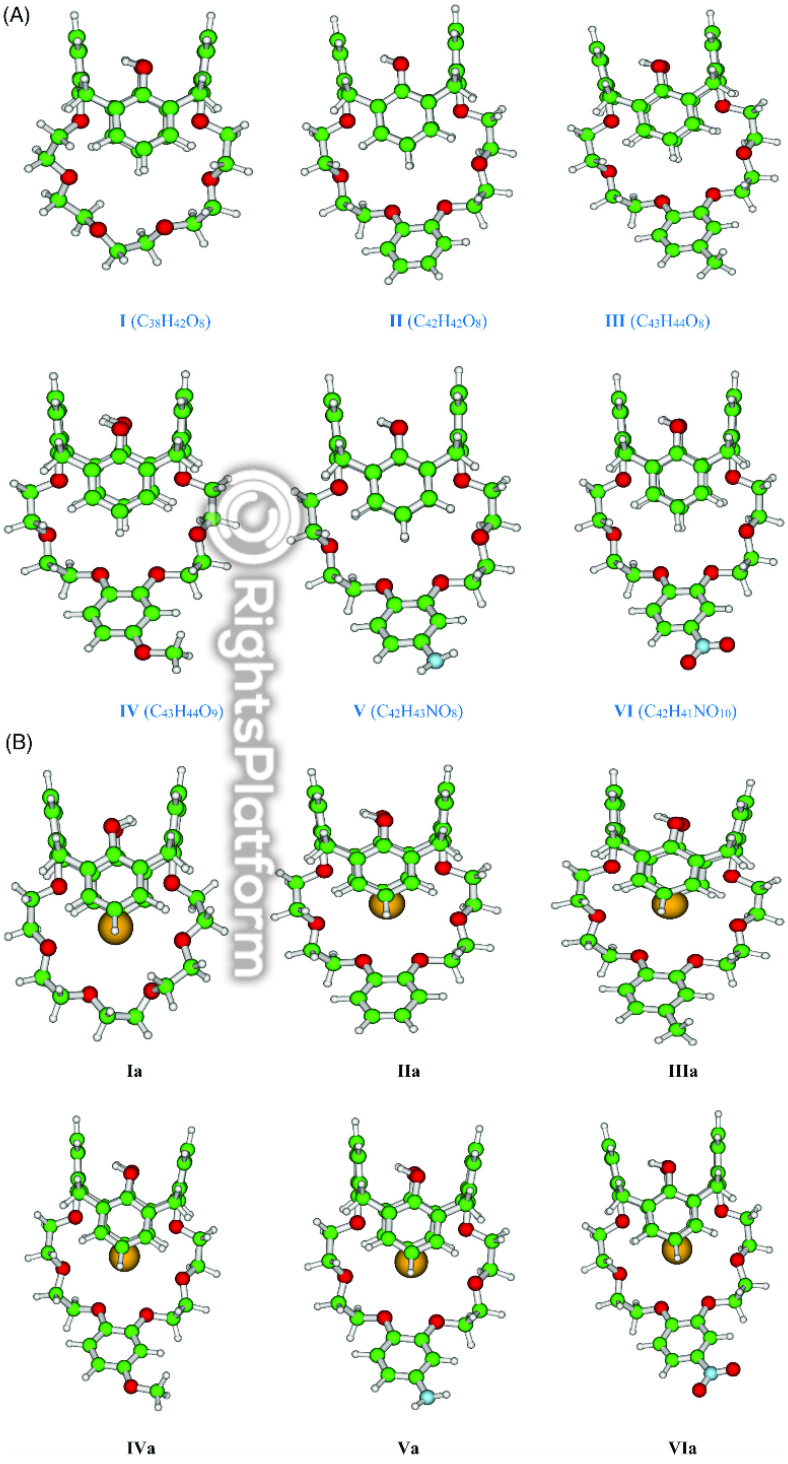

FIGURE 1 A, Optimized structures of calix[4]arene-crown-6 and substituted calix[4]arene-crown-6 at the B3LYP/TZVP level of theory. B, Optimized cesium complexes of calix[4]arene-crown-6 and substituted calix[4]arene-crown-6 at the B3LYP/TZVP level of theory

TABLE 1 Structural parameters of optimized free calix[4]arene crown-6 and substituted calix[4]arene crown-6 and Cs^+ complexes at the B3LYP/TZVP level of theory

		Free ligand		Cs-Complex	
S.No	Complex	C—O (A^0)	O—O (A^0)	C—O (A^0)	Cs^+—O (A^0)
1	**I**	1.388, 1.428, 1.417, 1.418, 1.419, 1.412, 1.415, 1.415, 1.414, 1.409, 1.431, 1.366	6.375, 6.547 7.094	1.402, 1.438, 1.423, 1.423, 1.4242, 1.422, 1.422, 1.421, 1.423, 1.419, 1.441, 1.382	3.283, 3.325, 3.384, 3.429, 3.300, 3.363
2	**II**	1.387, 1.427, 1.418, 1.414, 1.423, 1.361, 1.363, 1.425, 1.418, 1.414, 1.431, 1.378	6.237, 6.486, 6.887	1.401, 1.437, 1.424, 1.424, 1.430, 1.373, 1.374, 1.430, 1.425, 1.420, 1.442, 1.389	3.345, 3.386, 3.307, 3.364, 3.408, 3.204
3	**III**	1.378, 1.431, 1.414, 1.418, 1.424, 1.365, 1.362, 1.423, 1.415, 1.418, 1.427, 1.387	6.239,6.480, 6.899	1.389, 1.442, 1.420, 1.425, 1.429, 1.376, 1.374, 1.429, 1.424, 1.424, 1.437, 1.401	3.204, 3.408, 3.364, 3.302, 3.386, 3.348
4	**IV**	1.378, 1.432, 1.414, 1.418, 1.423, 1.369, 1.362, 1.422, 1.414, 1.418, 1.426, 1.387	6.247, 6.469, 6.894	1.401, 1.437, 1.425, 1.424, 1.428, 1.373, 1.380, 1.428, 1.425, 1.420, 1.442, 1.389	3.354, 3.383, 3.263, 3.397, 3.420, 3.205
5	**V**	1.387, 1.426, 1.418, 1.414, 1.422, 1.361, 1.370, 1.421, 1.419, 1.414, 1.432, 1.378	6.232, 6.471, 6.924	1.401, 1.437, 1.424, 1.424, 1.428, 1.373, 1.383, 1.426, 1.426, 1.419, 1.442, 1.388	3.359, 3.385, 3.253, 3.378, 3.420, 3.211
6	**VI**	1.388, 1.427, 1.419, 1.413, 1.429, 1.353, 1.350, 1.432, 1.415, 1.416, 1.431, 1.379	6.239, 6.513, 6.836	1.402, 1.437, 1.426, 1.424, 1.436, 1.365, 1.362, 1.435, 1.423, 1.422, 1.441, 1.390	3.306, 3.396, 3.388, 3.408, 3.393, 3.180

and 1.402 Å, whereas the C_{sp}^3 and O bond distances are increased to 1.424 to 1.442 Å. This increase in bond lengths between C and O is due to the interaction of O atoms with Cs metal ions. The Cs—O bond lengths are in the range of 3.283 to 3.429 Å, with an average distance of 3.347 Å. In the case of **II**, the C_{sp}^2 and O bond distance is 1.361 to 1.387 Å and C_{sp}^3, and O bond distances are 1.414 to 1.431 Å, similar to **I**. From the O—O bond distances of **I** and **II**, it is observed that the diagonal O-O distances are shorter in the case of **II** compared to **I**. In the complex **IIa**, the C_{sp}^2 and O bond distance is increased to 1.373 to 1.401 Å. The C_{sp}^3 and O bond distances are also increased to 1.424 to 1.442 Å. The Cs—O bond length is found to be within 3.204 to 3.408 Å, which is smaller than **Ia**. In the case of **III** and **IV**, the benzo group was further substituted with methyl and methoxy groups. On methyl and methoxy substitution, the C_{sp}^2 and O bond distances are found to be 1.362 to 1.387 Å, and C_{sp}^3 and O bond distances are 1.414 to 1.432 Å, similar to **II**.

From the O—O bond distances of **III** and **IV**, it is observed that the shorter value of the O—O bond distance of **III** is increased to 6.239 Å, and that of **IV** is increased to 6.247 Å compared to **II** (6.237 Å). Similarly, the longer O—O bond distance is also increased compared to **II**. The shorter and longer Cs—O bond distances of **IIIa** and **IVa** are 3.204 Å and 3.205 Å and 3.408 Å and 3.420 Å respectively. The Cs—O bond distances of **IVa** are longer compared to **II**. In the case of **V** and **VI**, the benzo group is substituted with amino and nitro groups, respectively. In the complexes **V** and **VI**, the C_{sp}^2 and O bond distances and the C_{sp}^3 and O bond distances are similar to that of **II**. From the O—O bond distances of **V** and **VI**, it is observed that the shorter value of O—O bond distance of **V** is decreased to 6.232 Å, and that of **VI** is increased to 6.239 Å compared to **II**, that is, 6.237 Å. Similarly, the longer O—O bond distance of **V** is increased to 6.924 Å and is decreased to 6.836 Å compared to **II**. The shorter and longer Cs—O bond distances of **Va** and **VIa** are 3.211 and 3.185 Å and 3.420 and 3.396 Å, respectively. The Cs—O bond distances of **Va** are higher compared to **II**, whereas for **Via**, it is shorter compared to **II**.

3.2 | Structure of 1,3-alternate diethoxy C4C6 and substituted 1,3-alternate diethoxy C4C6 and Cs^+ complexes

The structure of 1,3-alternate diethoxy C4C6 and their substituents are displayed in Figure 2. Structural parameters are given in Table 2. For the objectives of investigation, we have chosen 1,3-alternate diethoxycalix[4]arene-crown-6 ($C_{42}H_{50}O_8$), hereafter called **VII**; 1,3-alternatediethoxycalix[4]arenebenzo-crown-6 ($C_{46}H_{50}O_8$), **VIII**; 1,3-alternatediethoxycalix[4]arene-3′methylbenzo-crown-6 ($C_{47}H_{52}O_8$), **IX**; 1,3-alternatediethoxycalix[4]arene-3′methoxybenzo-crown-6 ($C_{47}H_{52}O_9$), **X**; 1,3-alternatediethoxycalix[4]arene-3′aminobenzo-crown-6 ($C_{46}H_{51}NO_8$), **XI**; **and** 1,3-alternatediethoxycalix[4]arene-3′nitrobenzo-crown-6 ($C_{46}H_{49}NO_{10}$), **XII**, and their complexes with Cs^+ metal ion are **VIIa**, **VIIIa**, **IXa**, **Xa**, **Xia**, and **XIIa**, respectively.

In the case of **VII**, the C_{sp}^2 and O bond distances are 1.383 and 1.386 Å, and C_{sp}^3 and O bond distances range from 1.414 to 1.427 Å. The diagonal O—O bond distances are also given in Table 2.

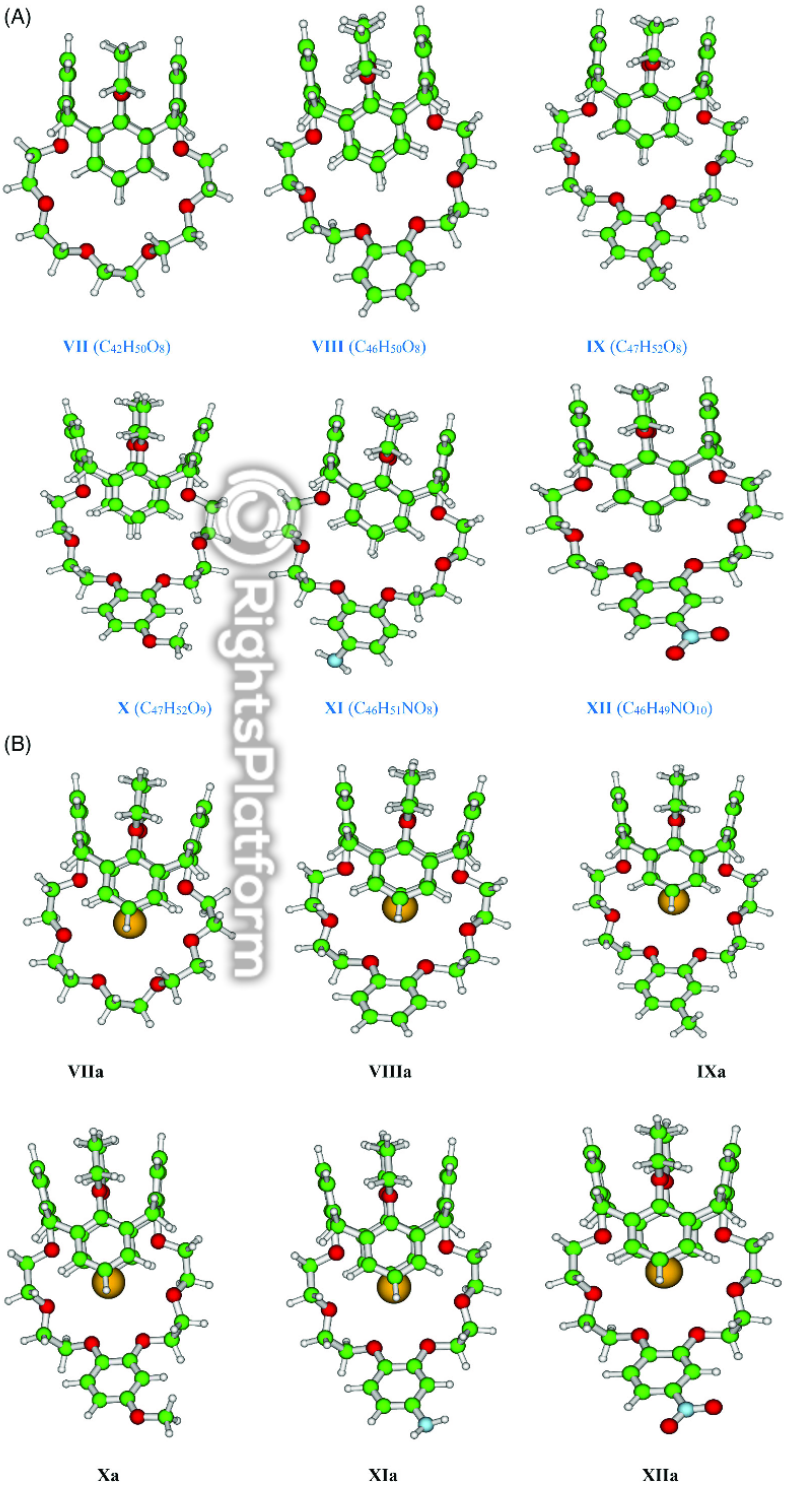

FIGURE 2 A, Optimized structures of 1,3-alternate diethoxycalix[4]arene-crown-6 and substituted 1,3-alternate diethoxycalix[4]arene-crown-6 at the B3LYP/TZVP level of theory. B, Optimized cesium ion complexes 1,3-alternate diethoxycalix[4]arene-crown-6 and substituted 1,3-alternate diethoxycalix[4]arene-crown-6 at the B3LYP/TZVP level of theory

TABLE 2 Structural parameters of optimized free 1,3-alternate diethoxycalix[4]arene-crown-6 and substituted 1,3-alternate diethoxycalix[4]arene-crown-6 and Cs^+ complexes at the B3LYP/TZVP level of theory

		Free calix		Cs-Complex	
S.No	Complex	C—O	O—O	C—O (A^0)	Cs^+—O (A^0)
1	**VII**	1.386, 1.427,1.415, 1.417, 1.419,1.414, 1.416, 1.417,1.415, 1.414, 1.425,1.383	6.721, 6.768, 6.825	1.401, 1.439,1.423, 1.424, 1.423,1.422, 1.422, 1.422, 1.421, 1.422, 1.438,1.395	3.266, 3.261, 3.439, 3.411, 3.321, 3.299
2	**VIII**	1.387, 1.426,1.417, 1.416, 1.424,1.363, 1.363, 1.427, .416, 1.416, 1.426,1.387	6.260, 6.381, 7.107	1.400, 1.438,1.423, 1.424, 1.429,1.373, 1.373, 1.430, 1.423, 1.422, 1.438,1.400	3.244, 3.351, 3.323, 3.401, 3.419, 3.211
3	**IX**	1.387, 1.426,1.416, 1.416, 1.426,1.365, 1.363, 1.424,1.416, 1.417, 1.426,1.387	6.255, 6.379, 7.114	1.400, 1.438,1.423, 1.424, 1.429,1.374, 1.375, 1.429, 1.423, 1.422, 1.438,1.400	3.248, 3.348, 3.315, 3.395, 3.416, 3.213
4	**X**	1.386, 1.431,1.420, 1.415, 1.421,1.362, 1.368, 1.423, .417, 1.416, 1.432,1.384	6.229, 6.631, 6.690	1.438, 1.400,1.424, 1.424, 1.428,1.374, 1.379, 1.429, 1.423, 1.421, 1.438,1.400	3.258, 3.346, 3.266, 3.419, 3.415, 3.222
5	**XI**	1.387, 1.426,1.417, 1.416, 1.424,1.363, 1.371, 1.423, .417, 1.415, 1.426,1.387	6.235, 6.382, 7.139	1.400, 1.438,1.423, 1.424, 1.428,1.374, 1.382, 1.427, 1.424, 1.421, 1.438,1.400	3.259, 3.351, 3.261, 3.396, 3.420, 3.226
6	**XII**	1.387, 1.426,1.418, 1.414, 1.430,1.355, 1.350, 1.434, .413, 1.418, 1.426,1.388	6.265, 6.408, 7.045	1.401, 1.438,1.425, 1.424, 1.435,1.365, 1.361, 1.435, 1.422, 1.425, 1.437,1.402	3.213, 3.346, 3.416, 3.441, 3.391, 3.188

In complex **VIIa**, the C_{sp}^2 and O bond distance is increased to 1.395 and 1.401 Å, whereas C_{sp}^3 and O bond distances are increased to 1.421 Å to 1.439 Å due to the interaction of O atoms with the Cs metal ion. The shorter and longer Cs—O bond lengths are 3.266 Å and 3.439 Å, respectively. In the case of **VIII**, the C_{sp}^2 and O bond distance is 1.363 Å to 1.387 Å, which is shorter than **VII**, whereas C_{sp}^3 and O bond distances range from 1.416 to 1.427 Å, similar to **VII**. The diagonal O—O bond distances are displayed in Table 2. From the O—O bond distances of **VII** and **VIII**, it is observed that the shorter O—O bond distance is further shortened and the longer O—O bond distance is further lengthened compared to **VII**. In the complex **VIIIa**, the C_{sp}^2 and O bond distance is increased to 1.373 Å to 1.401 Å, and the C_{sp}^3 and O bond distances are increased to 1.422 Å to 1.438 Å. The Cs—O bond length is shorter (3.211 Å) than VIIa and is longer (3.419 Å) than VIIa. In the case of **IX** and **X**, the benzo group was further substituted with methyl and methoxy groups. On methyl substitution, the C_{sp}^2 and O bond distances are changed to 1.363 Å to 1.387 Å, and C_{sp}^3 and O bond distances are elongated to 1.416 Å Å to 1.426 Å, similar to **VIII**. On methoxy substitution, the C_{sp}^2 and O bond distance is 1.368 Å to 1.387 Å, and the C_{sp}^3 and O bond distance is 1.415 Å to 1.431 Å. From the O—O bond distances of **IX** and **X**, it is observed that the shorter O—O bond distance of **IX** and **X** is decreased to 6.255 Å and 6.229 Å, respectively, compared to **VIII** (6.260 Å). Similarly, the longer O—O bond distance is increased for **IX** and decreased for **X** compared to **VIII**. The shorter and longer Cs—O bond distances of **IXa** and **Xa** are 3.213 Å and 3.222 Å and 3.416 Å and 3.419 Å, respectively. In the case of **XI** and **XII**, the benzo group is substituted with amino and nitro groups, respectively. From the O—O bond distances of **XI** and **XII**, it is observed that the shorter O—O bond distance of **XI** is decreased to 6.235 Å, and **XII** is increased to 6.265 Å compared to **VIII** (6.260 Å). Similarly, the longer O—O bond distance of **XI** is increased to 7.139 Å, and **XII** is decreased to 7.045 Å compared to **VIII**. The shorter and longer Cs—O bond distances of **XIa** and **XIIa** are 3.226 Å and 3.188 Å and 3.420 Å and 3.441 Å, respectively. The Cs—O bond distances of **XIa** are longer compared to **VIII** and **XII**a and are shorter compared to **VIII**.

3.3 | Metal ion-ligand binding energy

The gas-phase binding energy (BE) of a metal ion (M^+) with a ligand (L) can be expressed for the complexation reaction:

$$M^+{}_{(g)} + L_{(g)} \rightarrow M^+L_{(g)} \tag{2}$$

as

$$\Delta E = E_{M+L} - (E_{M+} + E_L) \tag{3}$$

TABLE 3 The calculated binding energies of Cs^+ ion with different calix systems

S. No	System	BE (B3LYP/TZVP)	Partial charge (a.u)	BE (MO6/TZ2P)
1	**I**	−57.12	0.9318	−75.45
2	**II**	−54.55	0.9387	−72.04
3	**III**	−55.02	0.9388	−72.16
4	**IV**	−55.07	0.9390	−72.63
5	**V**	−55.92	0.9390	−73.71
6	**VI**	−49.46	0.9386	−67.30
7	**VII**	−56.34	0.9316	−79.14
8	**VIII**	−53.24	0.9377	−73.06
9	**IX**	−53.66	0.9378	−73.56
10	**X**	−60.13(−89.96)[a]	0.9380	−77.19
11	**XI**	−54.50	0.9379	−74.34
12	**XII**	−48.26	0.9376	−67.72

[a]Indicates the binding energy value corresponding to Na^+ ion.

where E_{M^+L}, E_L, and E_{M+} represent the total energy of the complex, ligand, and the metal ion, respectively. The calculated BE values are given in Table 3. From the table, it is seen that BE of ligand **I** is −57.12 kcal/mol, which is reduced to −54.55 kcal/mol when **I** is substituted with the benzo group (**II**) due to the electron-withdrawing effect of benzo group. This can be well explained by natural bond order (NBO) analysis. From the NBO analysis, it is observed that the residual partial charge on Cs^+ in the case of **II**a is 0.9387, which is higher compared to **I**a (0.9318). This indicates that a less amount of charge is transferred from calixarene O atoms to Cs^+ in the case of **II**a. Addition of the methyl group to benzene ring (**III**) and methoxy group addition (**IV**) leads to a slight increase in BE by 0.5 kcal/mol. Similarly, addition of amino and nitro group resulted in **V** and **VI** ligands, and the corresponding complexes are **V**a and **VI**a, respectively. In the case of **V**a, the BE is increased by 1.37 kcal/mol compared to **II**a. The BE was decreased by 5.22 kcal/mol in the case of **VI**a compared to **II**a because of electron-withdrawing effect of the nitro group.

The BE of ligand **VII** is −56.34 kcal/mol, which, on substitution with the benzo group (**VIII**), was reduced to −53.24 kcal/mol due to the electron-withdrawing effect of the benzo group. It is seen from the NBO analysis that the residual charge on Cs^+ in **VIII**a is 0.9377, which is higher compared to **VII**a (0.9316). This indicates that a lesser amount of charge is transferred from Cs^+ to calixarene O atoms in the case of **VII**a. With the addition of the methyl group to the benzene ring (**IX**) and methoxy group (**X**), the BE is increased by 0.42 kcal/mol for **IX** compared to **VIII** and 6.89 kcal/mol for **X** compared to **VIII**. Similarly, addition of amino and nitro groups lead to **XI** and **XII** ligands, respectively, and the corresponding respective complexes are **XI**a and **XII**a. In the case of **XI**a, the BE is increased by 1.26 kcal/mol compared to **VIII**a. The BE was decreased by 4.98 kcal/mol in the case of **XII**a compared to **VIII**a because of the electron-withdrawing effect of the nitro group.

3.4 | Charge transfer

Electronic structure calculations are very useful to describe the host (C4C6)-guest (metal ion) type of interaction and thus helps in the design of tailor-made ion-selective ligands. Electronic chemical potential, μ, and absolute hardness, η, are generally used to characterize the chemical systems,[53] where

$$-\mu = \frac{(I+A)}{2} = \chi\eta = \frac{(I-A)}{2} \tag{4}$$

Here, I, A, and χ represent the ionization potential, electron affinity, and absolute electronegativity, respectively. According to Koopmans' theorem,[54] I and A can be obtained as

$$I = -E_{HOMO} A = -E_{LUMO} \tag{5}$$

The charge transfer amount, ΔN, can be calculated using[53]

$$\Delta N = \frac{(\chi^M - \chi^L)}{2(\eta^M + \eta^L)} \tag{6}$$

TABLE 4 Quantum chemical descriptors of calix[4]arene-crown-6 and substituted calix[4]arene-crown-6 at the B3LYP/TZVP level of theory

S. No	Complex	Charge on Cs(a.u)	E_{HOMO} (eV)	E_{LUMO} (eV)	ΔE (eV)	χ (eV)	η (eV)	ΔN
1	**I**	0.9318	−5.5788	−0.7343	4.84458	3.15654	2.42229	0.4836
2	**II**	0.9387	−5.6087	−0.7588	4.84994	3.18376	2.42497	0.4821
3	**III**	0.9388	−5.5662	−0.7465	4.81971	3.15630	2.40985	0.4842
4	**IV**	0.9390	−5.3006	−0.7479	4.55268	3.02424	2.27634	0.4979
5	**V**	0.9390	−5.07915	−0.7309	4.34824	2.90503	2.17412	0.5096
6	**VI**	0.9386	−5.76589	−2.4465	3.31938	4.1062	1.65969	0.4717

TABLE 5 Quantum chemical descriptors of 1,3 alternate diethoxy calix[4]arene-crown-6 and substituted1,3 alternate diethoxy calix[4]arene-crown-6 at the B3LYP/TZVP level of theory

S. No	Complex	Charge on Cs(a.u)	E_{HOMO} (eV)	E_{LUMO} (eV)	ΔE (eV)	χ (eV)	η (eV)	ΔN
1	**VII**	0.9316	−5.69462	−0.0710	5.62357	2.882835	2.811785	0.4785
2	**VIII**	0.9377	−5.70857	−0.1677	5.54087	2.938135	2.770435	0.4777
3	**IX**	0.9378	−5.5913	−0.1828	5.40842	2.88709	2.70421	0.4834
4	**X**	0.9380	−5.30564	−0.2644	5.04115	2.785065	2.520575	0.4977
5	**XI**	0.9379	−5.09667	−0.1083	4.98828	2.60253	2.49414	0.5084
6	**XII**	0.9376	−5.90243	−2.4568	3.44557	4.179645	1.722785	0.4643

Here, *M* stands for metal ion (acceptor), and *L* stands for ligand, that is, C4C6 (donor). The difference in energy of LUMO and HOMO, $\Delta E_{HL} = E_{LUMO} - E_{HOMO}$, provides the reactivity of chemical systems. Lower values of ΔE_{HL} represent higher reactivity and vice versa.

The calculated quantum chemical descriptors values are presented in Tables 4 and 5, and the HOMO and LUMO are given in Figure 3. In -Table 4, the descriptors of C4C6 and their substituents were provided. From the table, it is found that the charge transfer is the highest for **V** and the lowest for **VI**. The charge transfer in **I** is greater than **II**, and the same has been reflected in the higher BE of **I** than **II**. The values of ΔN on substitution with the methyl and methoxy and amino groups were increased and, on nitro substitution, were decreased compared to **II**. The same trend was observed in the BEs. The BE order was **V > IV > III > II > VI**, whereas the ΔN order was **V < IV < III < II < VI**. From the table, it is seen that the ΔE_{HL} value is the highest for **II** and lowest for **VI**. The ΔE_{HL} value of **I** is smaller than **II**, and the same has been reflected in the BE. That is, the BE of **I** is greater than **II**. By substituting methyl and methoxy and amino groups, the ΔE_{HL} values were decreased compared to **II**. The same trend was observed in the BEs. The BE order was **V > IV > III > II**, whereas the ΔE_{HL} order was **V < IV < III < II**. On nitro substitution, ΔE_{HL} was further decreased compared to **II**, and the BE was also decreased compared to **II**. Hence, no correlation can be drawn using the value of ΔE_{HL} on nitro substitution.

In Table 5, the descriptors of 1,3 alternate diethoxy C4C6 and their substituents were provided. From the table, it is found that the charge transfer is the highest for **V** and lowest for **VI**. The charge transfer in **I** is greater than **II**, and the same has been reflected in the BE, that is, the BE of **I** is greater than **II**. By substituting methyl and methoxy and amino groups, the values of ΔN were increased compared to **II** and on nitro substitution ΔN was decreased compared to **II**. The trend observed in the BE was **IV > V > III > II > VI**, whereas the trend in ΔN was **V < IV < III < II < VI**. The order in ΔE_{HL} was **VI < V < IV < III < II < 1**. We could not find any correlation for methoxy substitution from ΔN and ΔE_{HL}.

3.5 | Atoms in molecule calculations

In atoms in molecule (AIM) calculations, the charge density (ρ_c) and Laplacian ($\nabla^2\rho_c$) at bond critical point (BCP), where $\nabla\rho(r) = 0$, are used to describe the strength and characterization of bond.[55,56] The bigger ρ_c values describe stronger bonds. On the other hand, $\nabla^2\rho_c < 0$ represents a covalent bond, while $\nabla^2\rho_c > 0$ represents closed-shell interaction (ionic bond, coordination bond, hydrogen bond, or van der Waals interaction).

The calculated values of charge density (ρ_c) and Laplacian ($\nabla^2\rho_c$) at BCP are listed in Tables 6 and 7. From the calculated values of $\nabla^2\rho_c$, the interactions between donor atoms and metal ions were found to be closed-shell interactions because of their positive $\nabla^2\rho_c$ values. Furthermore, these interactions were stronger than the hydrogen bond from their ρ_c and $\nabla^2\rho_c$ values which are larger than that of hydrogen bond, for which ρ_c = 0.002 to 0.035 e/au^3 and $\nabla^2\rho_c$ = 0.024 to 0.139 e/au^5.[57] On the contrary, the ellipticity value ε of BCP reflects the characteristics of σ bond.[58] A large value of ε indicates a large deviation from the σ bond. The AIM parameters of complexes of C4C6 and substituted C4C6 are given in Table 6, and complexes of 1,3 alternate-diethoxy C4C6 and substituted 1,3 alternate-diethoxy C4C6 are given in Table 7. The BCP

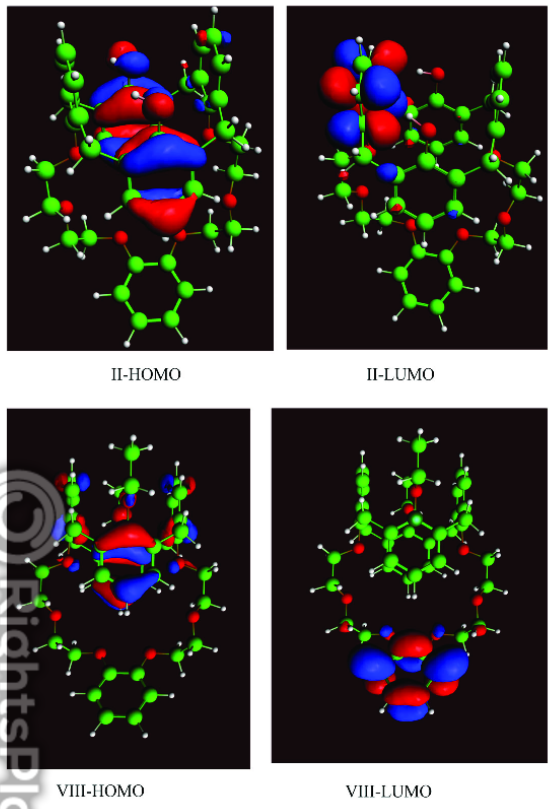

FIGURE 3 HOMO and LUMO of calix[4]arenebenzo-crown-6 and 1,3-alternate diethoxycalix[4]arenebenzo-crown-6

graphics are displayed in Figure 4. The calculated values shows that the interactions between metal ion and donor atoms were closed-shell interactions because of the positive values of $\nabla^2\rho_c$. On the contrary, the large value of ε indicates that the Cs^+ and O bonds have partial ionic character. In the case of Cs^+ complexes of substituted C4C6, it is observed that the average value of $\nabla^2\rho_c$ is greater for the complex **Va** (ie, 0.0340 e/au^5) compared to other complexes. This may be the reason for selectivity for Cs^+ with **Va** compared to other complexes. Similarly, in the case of complexes of 1,3 alternate-diethoxyC4C6 and substituted 1,3 alternate-diethoxyC4C6, the calculated values of $\nabla^2\rho_c$ are greater for **X** and **XIa** complexes, that is, 0.0351 e/au^5. Furthermore, the calculated value of ε indicates more ionic character in the **Xa** (0.0983) compared to **XIa** complex (0.0968). This may be the reason for the selectivity for Cs^+ with **Xa** complex compared to all other studied complexes of substituted C4C6 and substituted 1,3 alternate- diethoxy C4C6.

3.6 | Gibbs free energies of complexes in gas phase and different solvents

The Gibbs free energy (G) of the optimized metal-calix[4]arene complexes has been assessed using an earlier reported procedure.[28] The free energy of the complex is computed using thermodynamic cycle given in Figure 5.

3.6.1 | Gibbs free energies of Cs^+ complexes of C4C6 and substituted C4C6

The free energy of Cs^+ complex with C4C6 and substituted C4C6 are calculated in the gas phase and in solvents such as toluene, chloroform, octanol, and nitrobenzene are calculated and given in Table 8. The ΔG_{Cs} value was taken from our previous study.[28] The gas-phase free energy of complexation was found to be smaller than the gas-phase BE. This is due to the structure-making process of the complex formation. The gas-phase free energy of **IIa** is greater than **Ia**, but the BE is in the reverse order. This is due to the rigidity imparted to the C4C6 by the addition of

TABLE 6 AIM parameters of Cs^+ complexes of calix[4]arene-crown-6 and substituted calix[4]arene-crown-6 at the B3LYP/TZVP level of theory

Complex	BCP	$\lambda 1$	$\lambda 2$	$\lambda 3$	ρ_c	$\nabla^2\rho_c$	$\varepsilon = (\lambda 1/\lambda 2) - 1$
Ia							
	Cs-O1	−0.0059	−0.0052	0.0422	0.0074	0.0312	0.1346
	Cs-O2	−0.0072	−0.0063	0.0508	0.0088	0.0374	0.1429
	Cs-O3	−0.0067	−0.0063	0.0475	0.0085	0.0345	0.0635
	Cs-O4	−0.0056	−0.0053	0.0411	0.0074	0.0302	0.0566
	Cs-O5	−0.0051	−0.0049	0.0375	0.0069	0.0275	0.0408
	Cs-O6	−0.0067	−0.0060	0.0490	0.0085	0.0363	0.1167
IIa							
	Cs-O1	−0.0061	−0.0053	0.0440	0.0077	0.0326	0.1509
	Cs-O2	−0.0086	−0.0076	0.0607	0.0104	0.0445	0.1316
	Cs-O3	−0.0054	−0.0051	0.0392	0.0072	0.0287	0.0588
	Cs-O4	−0.0059	−0.0053	0.0426	0.0076	0.0314	0.1132
	Cs-O5	−0.0068	−0.0062	0.0486	0.0086	0.0355	0.0968
	Cs-O6	−0.0057	−0.0055	0.0413	0.0075	0.0302	0.0364
IIIa							
	Cs-O1	−0.0086	−0.0076	0.0607	0.0104	0.0445	0.1316
	Cs-O2	−0.0060	−0.0053	0.0437	0.0076	0.0324	0.1321
	Cs-O3	−0.0057	−0.0055	0.0413	0.0075	0.0302	0.0364
	Cs-O4	−0.0069	−0.0063	0.0491	0.0087	0.0359	0.0952
	Cs-O5	−0.0058	−0.0053	0.0426	0.0076	0.0314	0.0943
	Cs-O6	−0.0054	−0.0051	0.0392	0.0072	0.0287	0.0588
IVa							
	Cs-O1	−0.0086	−0.0076	0.0605	0.0104	0.0443	0.1316
	Cs-O2	−0.0059	−0.0052	0.0431	0.0075	0.0319	0.1346
	Cs-O3	−0.0058	−0.0055	0.0416	0.0076	0.0304	0.0545
	Cs-O4	−0.0076	−0.0069	0.0537	0.0094	0.0391	0.1014
	Cs-O5	−0.0054	−0.0049	0.0394	0.0071	0.0292	0.1020
	Cs-O6	−0.0052	−0.0050	0.0381	0.0070	0.0279	0.0400
Va							
	Cs-O1	−0.0059	−0.0051	0.0426	0.0074	0.0316	0.1569
	Cs-O2	−0.0085	−0.0075	0.0598	0.0102	0.0439	0.1333
	Cs-O3	−0.0052	−0.0050	0.0382	0.0070	0.0280	0.0400
	Cs-O4	−0.0056	−0.0051	0.0412	0.0074	0.0305	0.0980
	Cs-O5	−0.0078	−0.0071	0.0549	0.0096	0.0400	0.0986
	Cs-O6	−0.0057	−0.0055	0.0414	0.0075	0.0302	0.0364
VIa							
	Cs-O1	−0.0067	−0.0058	0.0480	0.0083	0.0352	0.1552
	Cs-O2	−0.0090	−0.0079	0.0633	0.0107	0.0468	0.1392
	Cs-O3	−0.0056	−0.0053	0.0405	0.0073	0.0296	0.0566
	Cs-O4	−0.0052	−0.0048	0.0385	0.0069	0.0285	0.0833
	Cs-O5	−0.0054	−0.0049	0.0393	0.0071	0.0297	0.1020
	Cs-O6	−0.0056	−0.0053	0.0410	0.0074	0.0295	0.0566

benzene ring, resulting in a more positive ΔS of complex **I**a than **II**a (given in the Table S1), leading to less free energy. The gas-phase free energies of **III**a and **IV**a are also lower than **II**a due to their large entropy difference compared to **II**a. The free energy of **VI**a is lower than **II**a in the gas phase. The free energy value of **V**a in the gas phase is higher compared to all studied complexes (6) here. The free energy in the solvent phase, ΔG_{ext}, of all the complexes were found to be positive in the toluene solvent. The ΔG_{ext} of **II**a is found to be higher in the chloroform solvent